ISSN : 0974 - 7486 Volume 7 Issue 6

Trade Science Inc.

Materials Science

An Indian Journal

Full Paper

MSAIJ, 7(6), 2011 [418-424]

Study of the matrix-carbide eutectic compound in carbon-rich 30wt.% cr-containing nickel, cobalt and iron-based hard alloys

Saidou Kane[1], Patrice Berthod[1,2*]

[1]Faculty of Sciences and Technologies, B.P. 70239, 54506 Vandoeuvre-lès-Nancy, (FRANCE)

[2]Institut Jean Lamour (UMR 7198), Department of Chemistry and Physics of Solids and Surfaces, B.P. 70239, 54506 Vandoeuvre-lès-Nancy, (FRANCE)

E-mail : Patrice.Berthod@ijl.nancy-universite.fr

Received: 23rd June, 2011 ; Accepted: 23rd July, 2011

ABSTRACT

Some of the wear-resistant tools or coatings are based on Ni, Co or Fe and contain very high carbon contents for promoting high volume fractions of carbides in the microstructures. Among them fine eutectic carbides and coarse pro-eutectic carbides do not induce the same properties for the alloys in terms of hardness, wear resistance and impact toughness. Thus it may be important to know in which proportions they are in the eutectic form and as coarse carbides. Eighteen 30wt.%-containing nickel-based, cobalt-based and iron-based alloys with six different carbon amounts (from 2.5 to 5.0wt.%) previously elaborated by high frequency induction melting were metallographically characterized in their as-cast condition and after heat-treatments at high temperature. More precisely their microstructures were quantified by image analysis in order to separate the surface fractions of the pro-eutectic phases (dendrites of matrix or carbides) from the eutectic compound. These results were thereafter compared to the ones issued from Thermo-Calc calculations concerning the eutectic solidification part.

INTRODUCTION

Nickel-based alloys obtained by solidification are used in numerous applications, notably the ones rich in chromium which are often considered for aeronautic "hot" mechanical pieces to which chromium brings good resistance against high temperature oxidation by gases or corrosion by molten salts. High levels of hardness can be achieved by adding great quantities of carbon[1-4], thanks to the high intrinsic hardness displayed by the $Cr_{23}C_6$, Cr_7C_3 or Cr_3C_2 carbides precipitated during solidification, which is favourable to a good resistance against wear phenomena. Cobalt-based alloys rich in chromium, also used for some hot parts in aeronautic and power generation turbines (e.g. the blade-supporting disks) but which can be also encountered in industry applications (e.g. the hot metallic tools used in glass fiberizing for wool fabrication), display good resistance against corrosion by hot gases or molten glass, and in presence of high amount in carbon they develop numerous carbides in their microstructures (chromium carbides, or other ones: WC or W_2C for example)[5]. Great volume of hard phases can be also obtained in the iron-based alloys family, for example in presence of great amounts in chromium and in carbon, leading to iron-based bulk materials[6] or hardfacing coatings[7] alloys available for applications requiring high levels of hardness or of wear resistance.

In such alloys the carbides issued from solidification can be of one or two morphologic types: eutectic or

hyper-eutectic. The eutectic carbides, fine and mixed with matrix, may favour homogeneity for the hardness properties at the microstructure scale, while the soft matrix dendrites (hypo-eutectic alloys) and the very hard coarse pro-eutectic carbides may favour, in contrast, very heterogeneous hardness distribution in the microstructure. It is thus important to measure – or to predict – the volume fractions of the {matrix + carbide} eutectic compound and of either the dendrites of matrix or the pro-eutectic carbides. The aim of this study, which concerns {chromium carbides} – rich alloys, is precisely to perform surface fractions' measurements using image analysis and to exploit thermodynamic calculations, to value the respective quantities of the pro-eutectic matrix or carbide (depending on the hypo- or hyper-eutectic character of alloys) and of the {matrix + carbides} eutectic compound.

EXPERIMENTAL

The alloys of the study are the high carbon ones which were elaborated in previous studies[8-10]: six Ni-30wt.%Cr-xC, six Co-30wt.%Cr-xC and six Fe-30wt.%Cr-xC alloys with x varying from 2.5wt.% to 5wt.% (Ni25, Co25 and Fe25 to Ni50, Co50 and Fe50). One can remind that all these alloys were elaborated by foundry from pure elements (nickel, cobalt, iron and chromium: Alfa Aesar, purity higher than 99.9 wt.%; carbon: graphite). In each case the melting of the pure elements together was performed under an inert atmosphere of 300 mbars of Argon, with fusion and solidification achieved in the copper crucible of a CELES high frequency induction furnace.

Each ingot was cut in four parts. One was kept in the as-cast condition while the three other parts were exposed to high temperature during 50 hours, one at 1000°C, one at 1100°C and one at 1200°C, then cooled in air. Each sample, as-cast or having been exposed to high temperature, were cut, embedded in a cold resin (Escil CY230 + HY956), and polished with SiC paper from 240 to 1200 grit, and finished using a 1µm diamond–paste. The microstructures of the as-cast or the aged alloys were observed, using these mounted samples, by electron microscopy (Scanning Electron Microscope: Philips, model XL30), in Back Scattered Electrons mode (acceleration voltage: 20kV). Several images were taken at different magnifications and masks were drawn to hide either the dendrites of matrix, or the coarse pro-eutectic carbides, in order to assess separately the surface fractions of the pro-eutectic carbides (or the dendrites of matrix) and the eutectic compound, by image analysis (software Adobe Photoshop CS).

In parallel thermodynamic calculations were performed for each of the eighteen compositions for the temperature at which, during cooling, the eutectic part of solidification is imminent (existing phases: liquid and pro-eutectic phase). Of course this temperature varies with the chemical composition of the alloy: it is given in TABLE 1.

TABLE 1 : Temperatures of eutectic solidification start according to Thermo-Calc calculations (determined for the appearance of the first crystal of carbide (hypo-eutectic alloys) or of matrix (hyper-eutectic alloys)

T_{eut} max (°C)	2.5C	3.0C	3.5C	4.0C	4.5C	5.0C
Nickel alloys	1295.12	1281.39	1264.89	1258.51	1248.59	1242.47
Cobalt alloys	1286.88	1279.63	1271.38	1257.76	1240.78	1220.00
Iron alloys	1285.93	1287.18	1286.56	1284.00	1279.38	1272.61

These calculations were performed using the N-version of the Thermo-Calc software[12] and a database containing the descriptions of the Ni-Cr, Ni-C, Cr-C and Ni-Cr-C systems[12-14], of the Co-Cr, Co-C, Cr-C and Co-Cr-C systems[14-19] and of the Fe-Cr, Fe-C, Cr-C and Fe-Cr-C systems[14, 16, 17, 20-23]. To convert these surface fractions, assumed to be equivalent to volume fractions, the following volume masses were used[24]: 6.97 g/cm^3 for the $M_{23}C_6$ carbides, 6.92 g/cm^3 for M_7C_3 and 6.68 g/cm^3 for M_3C_2 and 2.25 g/cm^3 for graphite. The densities of the liquid, and then of the future eutectic compounds (hypothesis done) were supposed to be close to the volume masses of the matrixes which are 8.12 g/cm^3 for the nickel-based matrix, 7.95 g/cm^3 for the cobalt-based matrix and 7.29 g/cm^3 for the iron-based matrix.

RESULTS AND DISCUSSION

As-cast and post-heat treatment microstructures of the alloys

The microstructures of the alloys were examined

Full Paper

using the SEM in BSE mode and their types after stabilization at high temperature and fast cooling by air quenching were characterized by X-Ray Diffraction.

The nickel alloys are all hypereutectic, with a {matrix+carbide} eutectic compound and coarse pro-eutectic carbides. In addition graphite is present in the three carbon-richest alloys Ni40, Ni45 and Ni50. After exposure to high temperature the carbides are mainly Cr_3C_2 in all alloys. However Cr_7C_3 are also present in the two lowest-carbon alloys: Cr_7C_3 with Cr_3C_2 in Ni25 at 1000 and 1100°C, and only Cr_7C_3 at 1200°C in Ni25 and Ni30.

The cobalt-based alloys are hypo-eutectic (Co25 and Co30: matrix dendrites + interdendritic {matrix+carbides} eutectic), almost eutectic (Co35) or hyper-eutectic (Co40 to Co50: {matrix+carbides} eutectic + coarse acicular pro-eutectic carbides). In all cases only the Cr_7C_3 carbides seem existing. The two carbon-richest alloys contain in addition some graphite particles.

The microstructures of the iron-based alloys are only composed of matrix and carbides (no graphite). The Fe25 alloy displays a microstructure still hypo-eutectic with presence of matrix dendrites in addition to the {matrix + carbide} eutectic. The Fe30 alloy is near eutectic and the Fe35, Fe40, Fe45 and Fe50 alloys are all hyper-eutectic with presence, in addition to the same {matrix + carbide} eutectic, of coarse and acicular pro-eutectic carbides. X-Ray Diffraction results showed that a mix of $Cr_{23}C_6$ and Cr_7C_3 carbides exists at 1000 and 1100°C in Fe25, and at 1000°C in Fe30. In contrast Cr_7C_3 is the single carbide present in the Fe25 at 1200°C, in Fe30 at 1100 and 1200°C, and in the four carbon-richest alloys at the three test temperatures. Seemingly there is no other phase present.

Measurement of the volume fraction of eutectic compound; comparison with calculated results

The microstructures of the alloys and their preparation for image analysis are illustrated by the selected micrographs presented in Figure 1 for the nickel alloys (two hyper-eutectic alloys: separation of the eutectic compound + eventually graphite coloured in black and the pro-eutectic carbides coloured in white), in Figure 2 for the cobalt alloys (eutectic + eventually graphite in black and matrix dendrites or pro-eutectic carbides in white) and in Figure 3 (eutectic in black and pro-eutectic carbides in white) for the iron alloys.

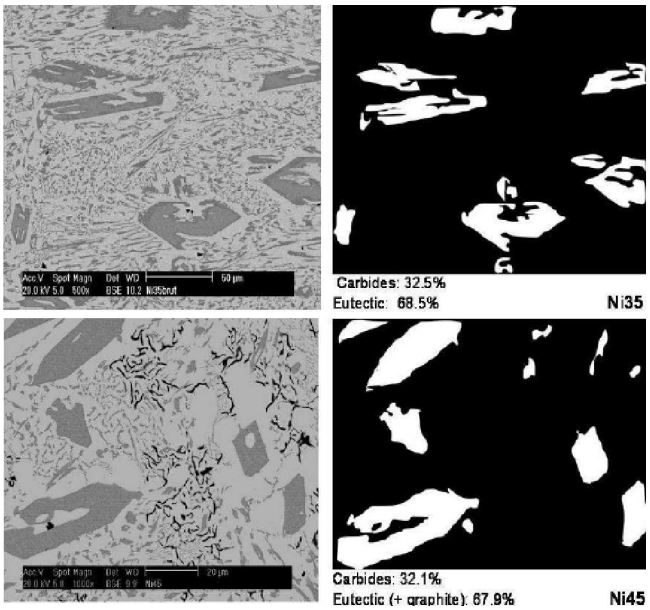

Figure 1 : Example of the microstructures observed on the nickel alloys and the masks drawn to isolate the eutectic compounds for image analysis; here: the as-cast Ni-30Cr-3.5C and Ni-30Cr-4.5C (wt.%) alloys

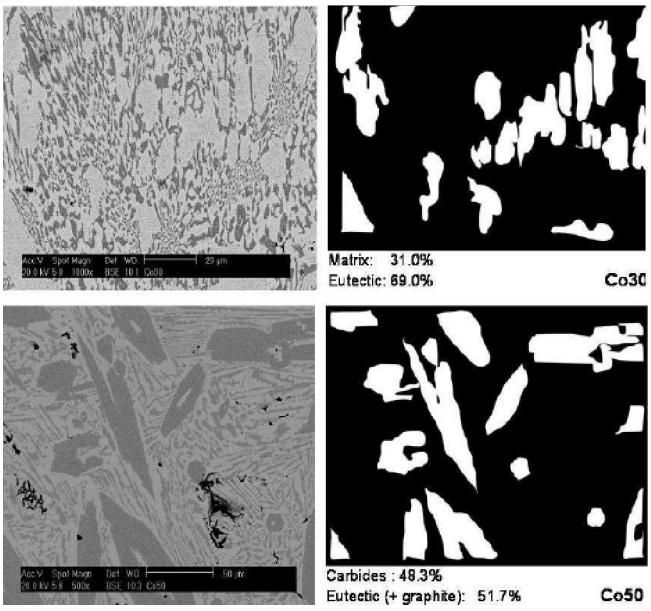

Figure 2 : Example of the microstructures observed on the cobalt alloys and the masks drawn to isolate the eutectic compounds for image analysis; here: the as-cast Co-30Cr-3.0C and Co-30Cr-5.0C (wt.%) alloys

The results of surface fractions of eutectic areas are plotted versus the carbon content in Figure 4, Figure 5 and Figure 6, respectively for the nickel alloys, cobalt alloys and iron alloys, graphs to which are also added

the calculated (Thermo-Calc) volume fractions of the residual liquid at the end of the pro-eutectic part of solidification. Concerning the surface fractions of eutectic two types of results were considered: first the values measured on the alloys in their as-cast states, and second the average value of the eutectic surface fractions measured for the three heat-treated states together, probably closer to what existed just after solidification.

For the nickel alloys, which are all hyper-eutectic, the calculated volume fractions of residual liquid then of eutectic compound, progressively decreases from about 90% to less than 80% while the fraction of pro-eutectic carbides increases from about 10vol.% to slightly more than 20vol.%. There is no such clear evolution for the values obtained by image analysis for the heat-treated alloys but these ones are rather close

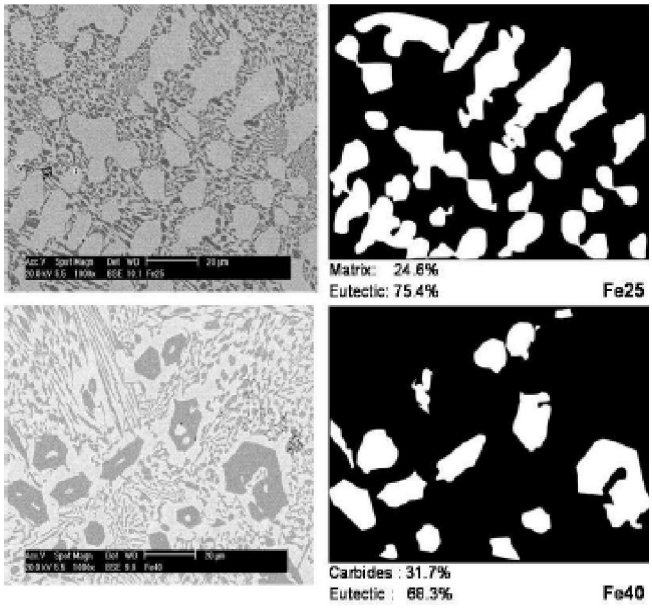

Figure 3 : Example of the microstructures observed on the iron alloys and the masks drawn to isolate the eutectic compounds for image analysis; here: the as-cast Fe-30Cr-2.5C and Co-30Cr-4.0C (wt.%) alloys

to the calculated ones. One must notice that the negligible contribution of graphite was not subtracted to the measured surface fractions of eutectic. The surface fractions of eutectic areas measured in the as-cast condition are slightly more different, a little lower.

For the cobalt alloys, which are hypo-eutectic for the C-poorest of them and hyper-eutectic for the C-richest of them, the calculated volume fraction of eutectic compound first increases to almost 100% (the carbon content is then very close to the eutectic value) then decreases down to about 80% when the carbides fraction increases up to about 20vol.%. In contrast with the nickel alloys, the surface fractions measured for the eutectic areas are significantly lower than the theoretical values (the negligible contribution of graphite being not subtracted). This is true for the heat-treated alloys as well as for the as-cast alloys.

For the iron alloys, which are also hypo-eutectic for the lowest carbon contents of this study and hyper-eutectic for the highest ones, calculations led to theoretic volume fractions of eutectic which increases up to almost 100% for 3wt.%C then decreases down to about 70vol.% for 5wt.%C. In the same time the theoretic volume fraction of carbides increases until reaching almost 30vol.% for 5wt.%C. The values deduced from image analysis are, here too, different from the theoretic volume fractions of eutectic, but the evolution versus the carbon content is more similar to the theoretic evolution than in the case of the cobalt alloys.

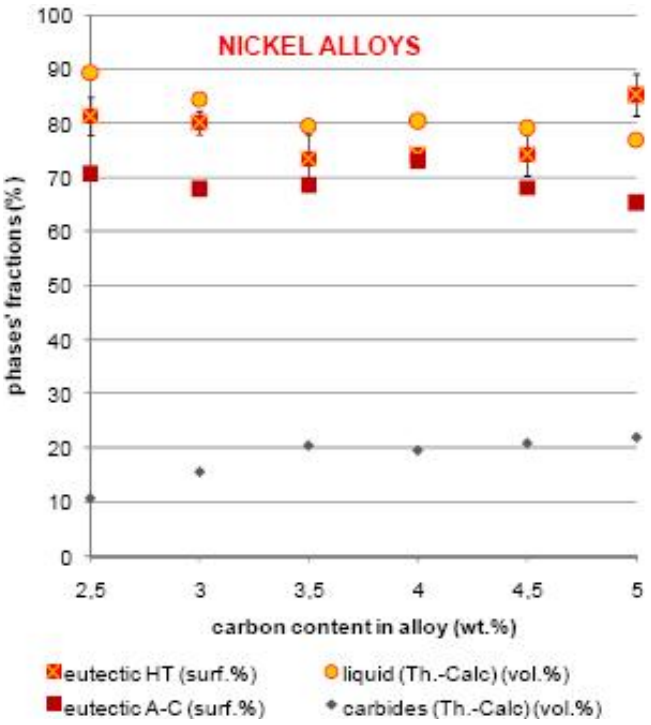

Figure 4 : Evolution of the volume fraction of eutectic compound, calculated and measured by image analysis of masked micrographs, versus the carbon content in the nickel alloys

General commentaries

Thus, masking the eutectic areas allowed to specify separately the real volume fractions of eutectic

compound in these eighteen alloys, as well as either their volume fractions of matrix dendrites or of pro-eutectic carbides. However, when the comparisons are done between the obtained results and the volume fractions issued from thermodynamic calculations after conversion of the calculated mass fractions at the solidus temperature, it appears that the agreement is not very good. It is rather good for the nickel alloys but discrepancies appeared concerning the cobalt alloys and the iron alloys. It is true that the unknown density of

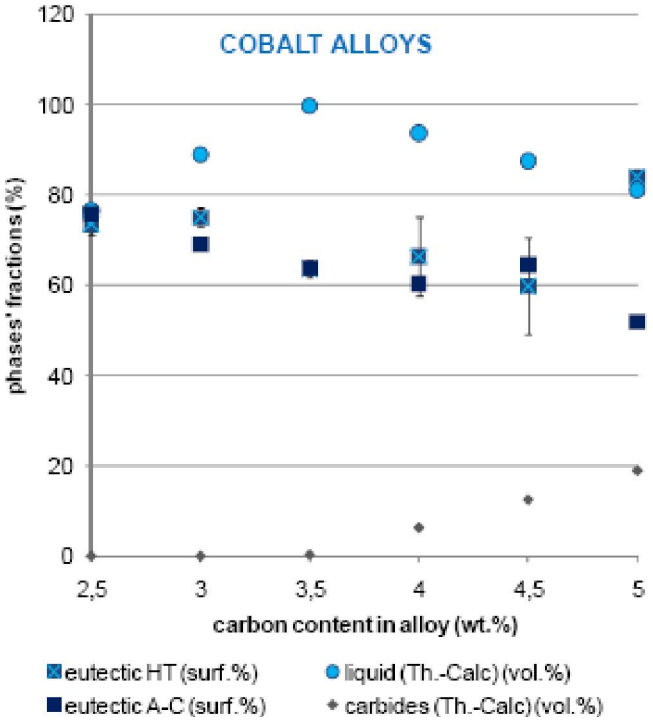

Figure 5 : Evolution of the volume fraction of eutectic compound, calculated and measured by image analysis of masked micrographs, versus the carbon content in the cobalt alloys

the residual liquid at the solidus temperature was supposed to be close to the matrix density in each case, an hypothesis which is probably not correct but which probably led to small mismatches only. The differences are more probably due to the masks drawings (not easy to do) which were not precise enough.

However one can try to exploit the results to deduce from the hardness of the carbides ($Cr_{23}C_6$: 1650Hv, Cr_7C_3: 1336Hv and Cr_3C_2: 1350 Hv)[24], the hardness of the eutectic compounds (for the Ni alloys, the almost eutectic Ni-30Cr-1.6C alloy: 308Hv_{30kg}; for the Co alloys, the almost eutectic Co-30Cr-3.5C one: 646Hv_{30kg}; and for the Fe alloys, the almost eutectic Fe-30Cr-3C one: 605Hv_{30kg}) if we can suppose that the matrix/carbides proportions are about the same in the eutectic compounds present in all the alloys of the same family (Ni-, Co- or Fe-based), and the hardness of the matrixes (Co-30Cr: 314Hv_{30kg} and Fe-30Cr: 184Hv_{30kg}), for determining, by a simple law of mixture using the volume fractions of these phases issued from Thermo-Calc calculations at the solidus temperature, the theoretic hardness of the studied alloys and make comparisons with the real ones measured by Vickers indentation under a load of 30kg.

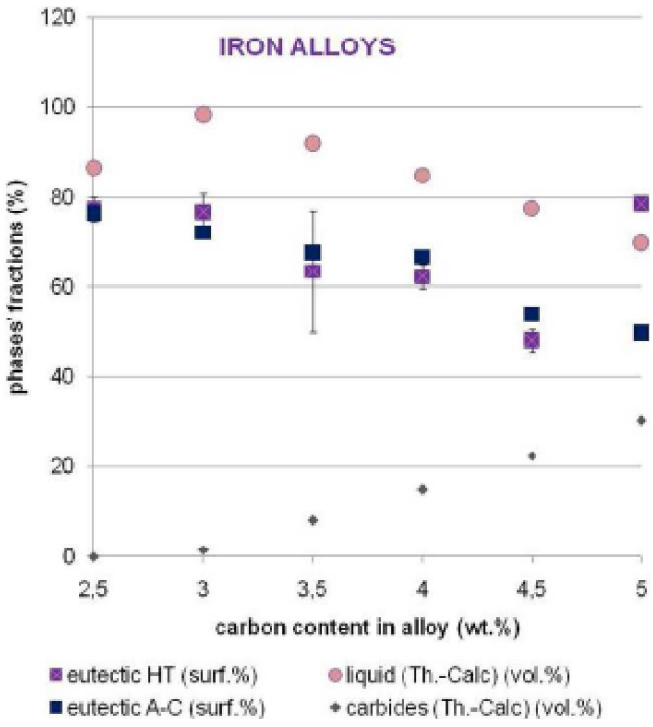

Figure 6 : Evolution of the volume fraction of eutectic compound, calculated and measured by image analysis of masked micrographs, versus the carbon content in the iron alloys

This gave the results graphically presented in Figure 7 in which one can see that there is a rather good agreement for the iron-based alloys and for the cobalt alloys (except for the highest carbon contents in which the softening phase graphite probably lowered the real hardness). There is also a serious but almost constant difference between the calculated hardness of the nickel alloys and the measured ones, with an enhancement of this mismatch for the highest carbon contents. This one can be also explained by the presence of the graphite in the three C-richest alloys. However there are, for these nickel alloys, similarities between the calculated hardness

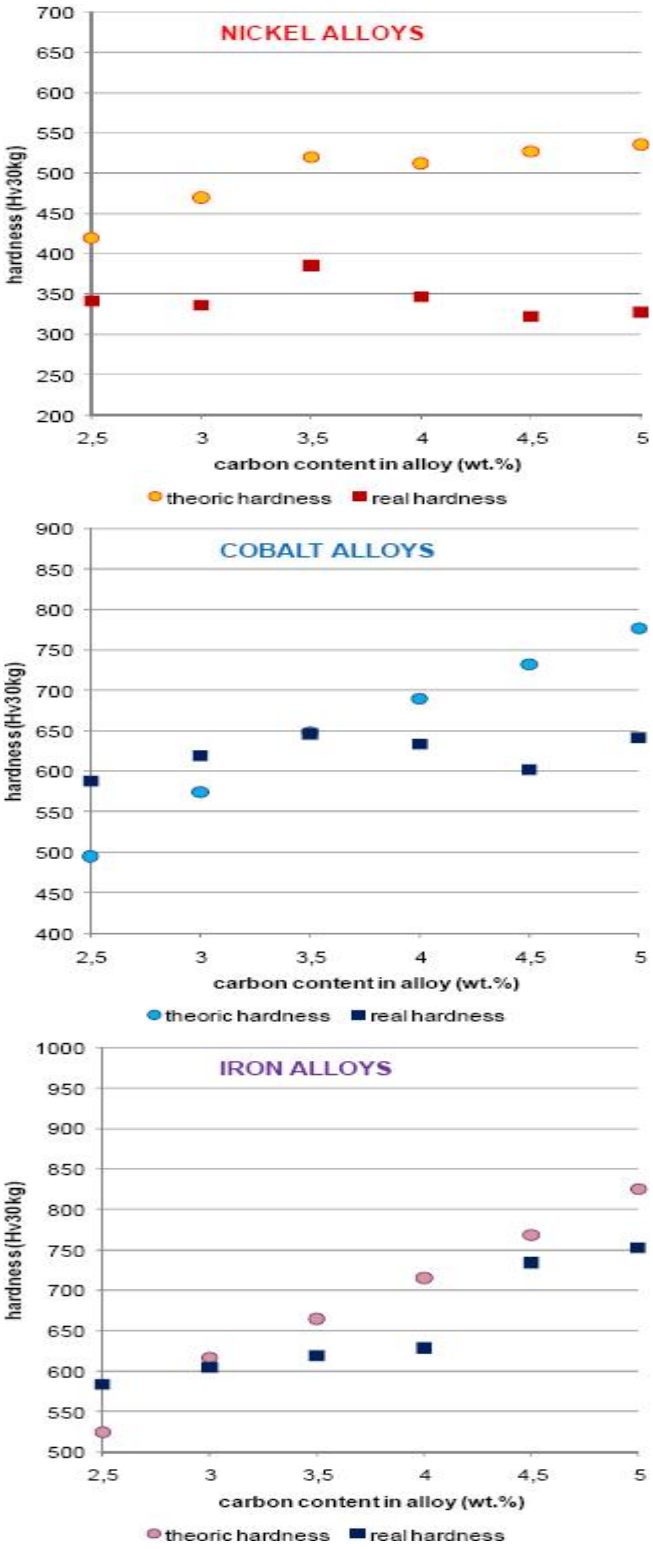

Figure 7 : Comparison between the theoretic hardness calculated from the calculated volume fractions of the different phases and their own hardness, and the measured hardness (all Ni-, Co- and Fe-based alloys in their as-cast conditions for the real hardness)

and the measured hardness, about the evolution of hardness versus the carbon content.

CONCLUSIONS

These ternary carbon-rich alloys based on nickel, cobalt or iron can be considered as eutectic alloys added with more or less soft dendrites of matrix or with hard pro-eutectic carbides (and also soft graphite in some cases) which induce a heterogeneous repartition of hardness. For a given chemical composition it is important to value the volume proportion of these pro-eutectic phases, which can be predicted by thermodynamic calculations by considering that the residual liquid existing just over the solidus temperature will give the eutectic compound. This can be also done by drawing masks on micrographs before performing surface fraction measurements by image analysis. This is unfortunately difficult to do and the obtained results can present mismatches with the calculated values, as met in this study for some alloys. However, such volume fractions of eutectic and of pro-eutectic phases allow evaluating the average hardness of the whole alloy, simply with a law of mixture based on these volume fractions and the hardness of the separated eutectic compound, matrix and carbides. This can give rather good values of this property which is of importance for estimate the wear resistance of these alloys.

ACKNOWLEDGEMENTS

The authors wish to thank Grégory Michel for his help for some thermodynamic calculations.

REFERENCES

[1] A.Klimpel, L.A.Dobrzanski, A.Lisiecki, D.Janicki; Journal of Materials Processing Technology, **164-165**, 1068 **(2005)**.
[2] Z.T.Wang, H.H.Chen; Mocaxue Xuebao Tribology, **25**, 203 **(2005)**.
[3] H.Han, S.Baba, H.Kitagawa, S.A.Suilik, K.Hasezaki, T.Kato, K.Arakawa, Y.Noda; Vacuum, **78**, 27 **(2005)**.
[4] D.Zhang, X.Zhang; Surface and Coating Technology, **190**, 212 **(2005)**.

[5] B.Roebuck, E.A.Almond; Int.Mater.Rev., **33**, 90 **(1988)**.
[6] H.E.N.Stone; Journal of Materials Science, **14**, 2781 **(1979)**.
[7] B.V.Cockeram; Metal and Materials Transactions A: Phys.Met.Mater.Sci., **33**, 3403 **(2002)**.
[8] P.Berthod, E.Souaillat, O.Hestin; Materials Science: An Indian Journal, **6(4)**, 260 **(2010)**.
[9] P.Berthod, O.Hestin, E.Souaillat; Materials Science: An Indian Journal, **7(1)**, 59 **(2011)**.
[10] P.Berthod, A.Dia, M.Ba; Materials Science: An Indian Journal, **7(3)**, 184 **(2011)**.
[11] Thermo-Calc Version N: "Foundation for Computational Thermodynamics" Stockholm, Sweden, Copyright **(1993, 2000)**.
[12] A.Dinsdale, T.Chart; MTDS NPL, Unpublished Work, **(1986)**.
[13] A.Gabriel, C.Chatillon, I. Ansara; High Temperature Science, **25**, 17 **(1988)**.
[14] J.O.Andersson; Calphad, **11**, 271 **(1987)**.
[15] A.Fernandez Guillermet; Int.J.Thermophys., **8**, 481 **(1987)**.
[16] J.O.Andersson; Int.J.Thermophys., **6**, 411 **(1985)**.
[17] P.Gustafson; Carbon, **24**, 169 **(1986)**.
[18] A.Fernandez Guillermet; Z.Metallkde, **78**, 700 **(1987)**.
[19] A.Fernandez Guillermet; Z.Metallkde., **79**, 317 **(1988)**.
[20] A.Fernandez Guillermet, P.Gustafson; High Temp.High Press., **16**, 591 **(1984)**.
[21] J.O.Andersson, B.Sundman; Calphad, **11**, 83 **(1987)**.
[22] P.Gustafson; Scan.J.Metall., **14**, 259 **(1985)**.
[23] J.O.Andersson; Met.Trans.A., **19A**, 627 **(1988)**.
[24] G.V.Samsonov; "Handbooks of High-Temperature Materials N°2, Properties Index", Plenum Press, New York **(1964)**.